Biodegradable Supramolecular Composites of Poly(ε-caprolactone) and Low-Molecular-Weight Organic Gelators

Mitsuhiro Shibata, Katsuyuki Kaneko, Kazuya Hirayama

Department of Life and Environmental Sciences, Faculty of Engineering, Chiba Institute of Technology, 2-17-1, Tsudanuma, Narashino, Chiba 275-0016, Japan

Received 19 April 2011; accepted 27 July 2011
DOI 10.1002/app.35365
Published online 29 November 2011 in Wiley Online Library (wileyonlinelibrary.com).

ABSTRACT: When a homogeneous hot liquid of poly(ε-caprolactone) (PCL) with (*R*)-12-hydroxystearic acid (HSA) or *N*-carbobenzyloxy-L-isoleucylaminooctadecane (CIA) was gradually cooled to room temperature, the mixture became gelatinous material and then solidified to give a PCL/HSA or PCL/CIA composite. The rheological measurements of the mixtures of PCL with HSA and CIA revealed that the organogels are formed at around 70–50°C and 100–73°C during the cooling process, respectively. Furthermore, the formation of supramolecular fibrillar networks was confirmed by the microscopic and differential scanning calorimetric analyses. The tensile moduli of both the composites were improved by the addition of CIA and HSA. Both the composites showed so high biodegradability as PCL. The fibrillar networks of the composites were also regenerated during the repeated cooling process from the isotropic liquid. © 2011 Wiley Periodicals, Inc. J Appl Polym Sci 124: 4165–4173, 2012

Key words: biodegradable; composites; self-assembly; polycaprolactone; organogelator

INTRODUCTION

The development of biodegradable polyesters such as polylactide (PLA), poly(butylene succinate) (PBS), poly(hydroxybutylate-*co*-valerate) (PHBV), and poly(ε-caprolactone) (PCL) has attracted increasing attention owing to the environmental problem induced by the accumulation of plastic waste.[1–3] However, large-scale application of the biodegradable polyesters limited up to now because of inferior thermal and mechanical properties to popular non-biodegradable polymers, as well as their relatively high price. As environmentally benign reinforcing methods of the biodegradable polyesters, the composites with layered silicate (nanocomposites)[4–9] have been the subject of many recent publications. The nanocomposites often exhibit properties superior to conventional composites, such as stiffness, thermal stability, barrier properties, as well as flame retardant behavior. However, the environmental and toxicological implications of such nano-sized fillers and the derived nanocomposites are not fully understood,[9] and the influence of the organically modified layered silicate on the biodegradability is still controversial.[4,6] Also, the manufacturing costs remain a significant factor restricting the growth of the application of the nanocomposites.[9]

Recently, we had reported a new supramolecular composite of castor oil-modified ε-caprolactone oligomer (CO-PCL) and fibers formed by the self-assembly of (*R*)-12-hydroxystearic acid (HSA).[10] HSA is a low-molecular-weight organic gelator (LMOG) which is derived from castor oil, and is widely used as a gelator of cooking oils. To extend an application range of the supramolecular composites, the uses of industrially available PCL and a LMOG other than HSA are examined in this study. Amino acid derivatives such as *N*-carbobenzyloxy-L-isoleucylaminooctadecane (CIA), *N*-lauroyl-L-glutamic acid-α,γ-bis(*n*-butylamide), N^{α}-acetyl-N^{ε}-dodecyl-L-lysine are known as powerful and environmentally benign LMOG in a similar manner to HSA.[11–18]

The present work describes the supramolecular composites of PCL with self-assembled HSA and CIA. The thermal and mechanical properties of the PCL/HSA and PCL/CIA composites are compared with those of a blend of PCL and stearic acid (STA) without gelating ability (Fig. 1). Aimed at the development of fully biodegradable and remendable fiber-reinforced plastics, the biodegradability of the supramolecular composites and the regeneration of the LMOG-based fibrillar network by repeated heat treatment are investigated in detail.

Correspondence to: M. Shibata (shibata@sky.it-chiba.ac.jp).
Contract grant sponsor: KAKENHI; contract grant number: 20550194.

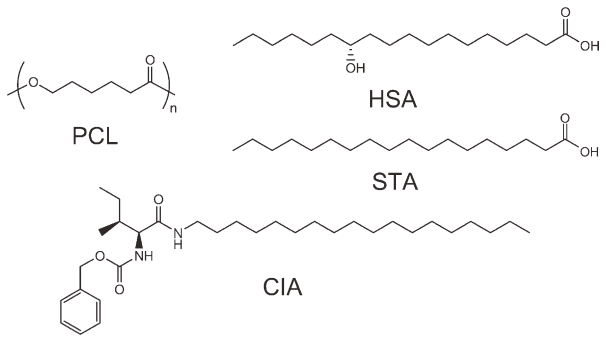

Figure 1 Structure of PCL, HSA, CIA, and STA.

EXPERIMENTAL

Materials

PCL (CelGreen P-H7®, density 1.14 g/cm^3, melt flow rate (190°C, 2.16 kg) 1.7 g/10 min) was supplied from Daicel (Osaka, Japan). HSA was kindly supplied from Itoh Oil Chemicals, Yokkaichi, Japan. *N*-Carbobenzyloxy-L-isoleucine was purchased from Watanabe Chemical Industries, Hiroshima, Japan. Stearic acid (STA, mp. 70°C) and 1-aminooctadecane were purchased from Tokyo Chemical Industry, Tokyo, Japan. Soybean oil (SBO) and *N*,*N*′-dicyclohexylcarbodiimide were purchased from Wako Chemical, Tokyo, Japan. All the other chemicals used in this work were reagent grade and used without further purification.

Synthesis of CIA

To a solution of *N*-carbobenzyloxy-L-isoleucine (2.51 g, 9.46 mmol) in dichloromethane (300 mL) was added *N*,*N*′-diisopropylcarbodiimide (1.19 g, 9.46 mmol) at 0°C. After the mixture was stirred for 1 h, 1-aminooctadecane (2.55 g, 9.46 mmol) was added and the mixture was stirred for 1 h at 0°C. Furthermore, the reaction mixture was stirred for 24 h at room temperature, and then stirred for 24 h at 35°C. The formed precipitate was filtered off, washed with dichloromethane (100 mL), and then dried *in vacuo* at 35°C for 24 h to give CIA as white powder (3.26 g) in 67% yield: mp. 112°C (lit. 113–114°C).[12] ^{1}H NMR ($CDCl_3$) δ 7.35 (s, 7H), 5.10 (s, 2H), 3.95 (d, 1H), 3.24 (m, 2H), 1.87 (bs, 1H), 1.48 (bm, 3H), 1.25 (s, 30H), 1.12 (m, 1H), 0.89 (m 9H).

Preparation of SBO/HSA and SBO/CIA organogels

As a control, SBO organogelators containing HSA 10 parts per hundred parts (phr) by weight of resin and CIA 10 phr were prepared as follows: HSA or CIA (5.00 g) was dissolved in SBO (50.0 g) at ca. 100 and 130°C, and then gradually cooled to room temperature to give SBO/HSA and SBO/CIA organogels containing HSA and CIA 10 phr (SBO/HSA10 and SBO/CIA10).

Preparation of PCL/HSA and PCL/CIA composites

A mixture of PCL (15.00 g) and HSA (0.75 g) was heated to 100°C and stirred for 15 min to give a homogeneous liquid. The hot oily substance was poured on a set of 10 molds kept at 100°C, which is composed of a stainless steel plate (250 × 200 × 2 mm^3) with 10 rectangular holes (45 × 10 mm^2), a poly(tetrafluoroethylene) film (250 × 200 × 0.10 mm^3) and a stainless steel plate (250 × 200 × 3 mm^3), piled in that order. After PCL/HSA was injected in the molds, a poly(tetrafluoroethylene) film (250 × 200 × 0.10 mm^3) and a stainless steel plate (250 × 200 × 3 mm^3) were covered and molded at pressure of 3 MPa and temperature of 100°C. The molds were cooled from 100°C to room temperature over 3.5 h, 10 rectangular specimens (45 × 10 × 1.8 mm^3) of PCL/HSA with HSA content 5 phr were taken out of the mold. The sample was abbreviated as PCL/HSA5. In a similar manner, PCL/HSA composites with HSA content 10 and 15 phr (PCL/HSA10 and PCL/HSA1015) and PCL/STA blend with STA 10 phr (PCL/STA10) were prepared. Also, the PCL/CIA composites with 5, 10, and 15 phr CIA (PCL/CIA5, PCL/CIA10, and PCL/CIA15) were prepared in a similar manner to PCL/HSA5, PCL/HSA10, and PCL/HSA15 except for using the mixing temperature at 130°C instead of 100°C.

Measurements

The differential scanning calorimetry (DSC) was performed on a Perkin-Elmer Diamond DSC in a nitrogen atmosphere. The samples cut from the compression-molded specimens were heated from −100 to 100°C at a rate of 20°C/min. Dynamic mechanical analysis (DMA) of a rectangular plate (30 × 5 × 1.8 mm^3) cut from the molded specimen was performed on a Rheolograph Solid (Toyo Seiki, Tokyo, Japan) with a chuck distance of 20 mm, a frequency of 1 Hz and a heating rate of 2°C/min. Tensile tests of the molded specimens were performed at 20°C using an Autograph AG-1 (Shimadzu, Japan). Span length was 30 mm, and the testing speed was 1 mm/min. Five composite specimens were tested for each set of samples, and the mean values were calculated. Rheological measurement was performed on a DAR-10 rheometer (REOLOGICA Instruments, Bordentown, NJ), using a plate type rotor of diameter of 20 mm. The measuring temperature was from 85 or 130°C at a cooling rate of 1°C/min. Sampling amount, sample load, and frequency were ca. 0.6 g, 2.4 N, and 1 Hz, respectively. Polarized and normal optical microscopy was performed on an Olympus BXP microscope equipped with crossed polars, a

Sony CCD-IRIS color video camera interfaced to a computer, and a Japan High-tech hot-stage RH-350. The samples were heated to 85 or 130°C on the hot-stage, held at the temperature for 3 min, and cooled to a temperature where the growing of fibrillar networks or micro-crystals starts at a cooling rate of 1°C/min. The samples cooled to room temperature was again heated to 85 or 130°C, held at the temperature for 3 min, and cooled at the same condition as the first cooling process in order to evaluate the regeneration of the supramolecular fibrillar network. Biodegradability was determined according to JIS K6950-2000 (ISO 14851-1999) by measuring a biochemical oxygen demand (BOD) in the aerobic aqueous medium containing activated sludge. Phosphate buffer (pH 7.4, 200 mL) containing 0.25 m*M* $CaCl_2$, 0.09 m*M* $MgSO_4$, 0.09 m*M* NH_4Cl, and 0.9 μ*M* $FeCl_3$ was mixed in a glass bottle. To the mixture, 4.35 mL of activated sludge containing 30 mg insoluble part, which was obtained from sewerage facilities of Chiba Institute of Technology, and 20 mg of the sample pulverized after immersion in liquid nitrogen were added. The dispersion was steadily stirred with a magnetic stir bar. BOD was measured at 25°C by using BOD tester 200F (Taitec Corporation, Koshigaya, Saitama, Japan). Carbon dioxide was absorbed into 50% sodium hydroxide aqueous concentrate in a cup equipped within the glass bottle. The volume of the consumed oxygen was directly measured with a scaled cylinder.

RESULTS AND DISCUSSION

Characterization of gelation for PCL/HSA and PCL/CIA by means of rheological analysis

To confirm the formation of organogel during the cooling stage of PCL/HSA and PCL/CIA samples, the rheological measurement was performed. When the PCL/HSA samples were cooled from 85°C, the elastic modulus (G') of liquefied sample rapidly increased around 70–50°C to ca. 10^5–10^6 Pa and again increased around 50–43°C [Fig. 2(a)]. The first increase of G' is due to an increase of viscosity related to the formation of HSA organogel. The temperature at which the G' starts to rise increased with increasing content of HSA. The second increase of G' is due to the crystallization of PCL. In case of PCL itself, the G' rapidly rose at 40°C due to the crystallization, indicating that the formation of HSA organogel promotes the crystallization of PCL component. The PCL/CIA showed a similar rheological behavior to PCL/HSA, as is shown in Figure 2(b). The G' of PCL/CIA rapidly increased at around 100–73°C on a cooling process, and again increased around 53–43°C. The temperature at which the G' starts to rise increased with increasing content of CIA. The second increase of G' is due to the crystallization of PCL. As a comparison, the rheological behavior of PCL/STA which does not gelate but crystallize was investigated. When the PCL/STA samples were cooled from 85°C, G' of liquefied sample increased a little around 65–55°C to ca. 10^5–10^4 Pa and again increased around 52–42°C [Fig. 2(c)]. The extent of

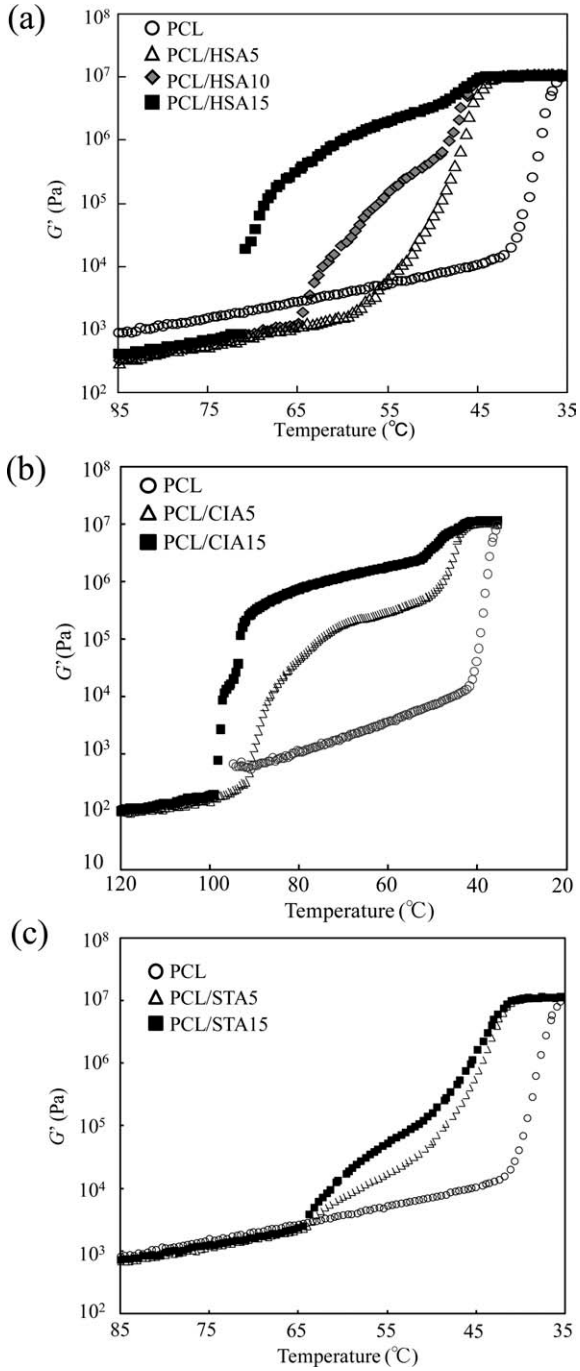

Figure 2 Temperature dependency of G' at a cooling rate of 1°C/min for (a) PCL and PCL/HSA composites; (b) PCL and PCL/CIA composites; and (c) PCL and PCL/STA blends.

increase of G' for PCL/STA was much less than those of PCL/HSA, because the former is not homogeneous gelation but heterogeneous crystallization containing isotropic PCL liquid phase. The temperature where G' starts to increase did not change by the content of STA, which was a little lower than the melting point of STA (70°C). The G' at 85°C for PCL/STA is a little lower than that of PCL and higher than that of PCL/HSA, suggesting that miscibility of STA toward PCL is lower than that of HSA. What the crystallization temperature of STA is little affected by STA content should be caused by a heterogeneous morphology of PCL and STA.

Characterization of PCL/HSA and PCL/CIA composites by means of optical microscopic analysis

Figure 3 shows polarized and normal optical photomicrographs of PCL/HSA10 and PCL/STA10 during the cooling process at a rate of 1°C/min from 85°C, and those of PCL/CIA10 and SBO/CIA10 during the same cooling process from 130°C. A typical organogel of SBO/CIA10 exhibited birefringence to some extent at 74°C under polarized light and fibrous aggregates were formed as are obvious from the normal optical micrograph. The PCL/CIA10 displayed similar birefringence at 85°C under polarized light and fibers with high aspect ratio were densely formed. The formation of fibers was also observed for PCL/HSA10 at 63°C. In contrast to these observations, typical crystalline texture was observed for PCL/STA10 at 58°C under polarized light and platelike morphology was observed on the normal optical micrograph.

Figure 4 shows polarized optical photomicrographs of PCL/HSA10 and PCL/CIA10 during the cooling stage at a rate of 1°C/min and the subsequent heating stage from 40°C at a rate of 1°C/min. When PCL/HSA10 was cooled from 85°C at which the sample is isotropic liquid, fibrous network started to form at around 63°C, and then crystallization of PCL occurred at around 40°C. We could not clearly see the fibrous network in the polarized optical photomicrograph of 40°C, because of the presence of PCL micro-crystals. However, when the sample was again heated at a rate of 1°C/min from 40°C, fibrous network could be seen at around 60°C which is near the T_m of PCL. This result shows that the fibrous network which was formed during the cooling process is maintained after the crystallization of PCL. A similar trend was observed for PCL/CIA10, as is obvious from Figure 3. The fibrous network of PCL/CIA10 was appeared at 85°C, can not be identified at 40°C because of the crystallization of PCL on the cooling process, and can be seen again at 85°C on the subsequent heating process.

Characterization of PCL/HSA and PCL/CIA by means of DSC and DMA

Figure 5 shows the first heating DSC thermograms of HSA, PCL/HSA5, PCL/HSA 10, PCL/HSA 15, and PCL. The melting temperature (T_m) of HSA and PCL was observed at 76.8°C ($\Delta H_m = 174$ J/g) and 63.3°C ($\Delta H_m = 76.9$ J/g), respectively. A broad endothermic peak was observed for PCL/HSA5 and PCL/HSA10 at 57.9°C ($\Delta H = 80.7$ J/g-PCL) and 59.8°C ($\Delta H = 79.2$ J/g-PCL), respectively, while no endothermic peak was observed at the region near T_m of HSA. These observations indicate that the broad endothermic peak contains both the melting of PCL crystalline phase and the isotropization of HSA mesogenic phase. In case of PCL/HSA15, T_m of HSA component was observed at 76.2°C ($\Delta H_m = 107$ J/g-HSA), suggesting that excess HSA crystallized.

Figure 6 shows the first heating DSC thermograms of PCL/CIA5, 10, 15. All the PCL/CIA composites showed a broad and weak endothermic peak at 94.9–102°C in addition to a strong endothermic peak due to the melting of PCL crystalline phase at 59–61°C. The temperature of the weak peak is lower than T_m of CIA (112°C), suggesting the formation of supramolecular mesophase of CIA molecules. The isotropization temperature (T_i) and its change of enthalpy (ΔH_i) of PCL/CIA samples increased with increasing amount of CIA, suggesting the CIA aggregates are more densely packed. However, as ΔH_i of PCL/CIA was much lower than ΔH_m of CIA, considerable amounts of CIA are dissolving in the PCL matrix.

Figure 7 shows DMA charts of the PCL, PCL/HSA10, PCL/CIA10, and PCL/STA10. The tan δ peak temperature corresponding to glass transition temperature (T_g) for PCL/HSA10, PCL/CIA10, and PCL/STA10 was the same as that of PCL (−58°C), indicating that HSA, CIA, and STA are almost immiscible to PCL at around the glass transition temperature (T_g) of PCL. The storage modulus (E') over the whole temperature range for PCL/HSA10 and PCL/CIA10 was higher than that for PCL, suggesting the reinforcement effect due to the formation of HSA and CIA-based fibers with high aspect ratio. In contrast to this result, the E' for PCL/STA10 was lower than that for PCL.

Figure 8 shows the E' at 20°C measured by DMA for PCL/HSA, PCL/CIA, and PCL/STA. The E' for PCL/CIA increased with increasing CIA content. Although, the E' for PCL/HSA also increased with increasing HSA content, the E' decreased at HSA content 15 phr because of the heterogeneous

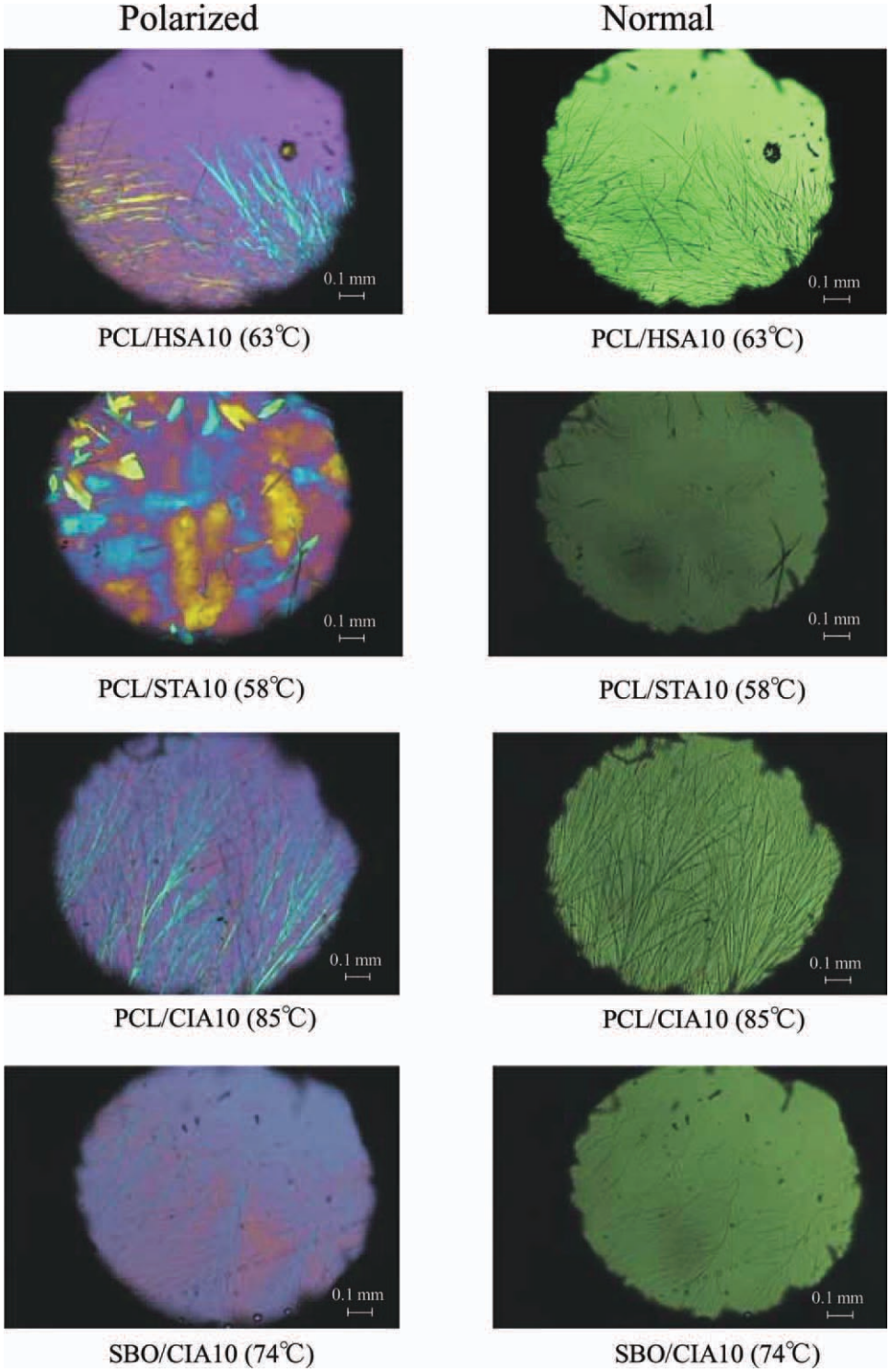

Figure 3 Polarized and normal optical photomicrographs of PCL/HSA10, PCL/STA10, PCL/CIA10, and SBO/CIA10 at the specified temperature during the cooling stage at a rate of 1°C/min. [Color figure can be viewed in the online issue, which is available at wileyonlinelibrary.com.]

crystallization of HSA. What E' of PCL/CIA was higher than that of PCL/HSA should be related to the higher density of fibrous network for PCL/CIA10, as is obvious from the optical micrographs shown in Figure 3. In contrast to the increase of E' for PCL/HSA and PCL/CIA, the addition of STA to PCL caused a decrease of E'. It means that the rigidity of the composite is not improved by a simple heterogeneous crystallization of low molecular-weight organic compound.

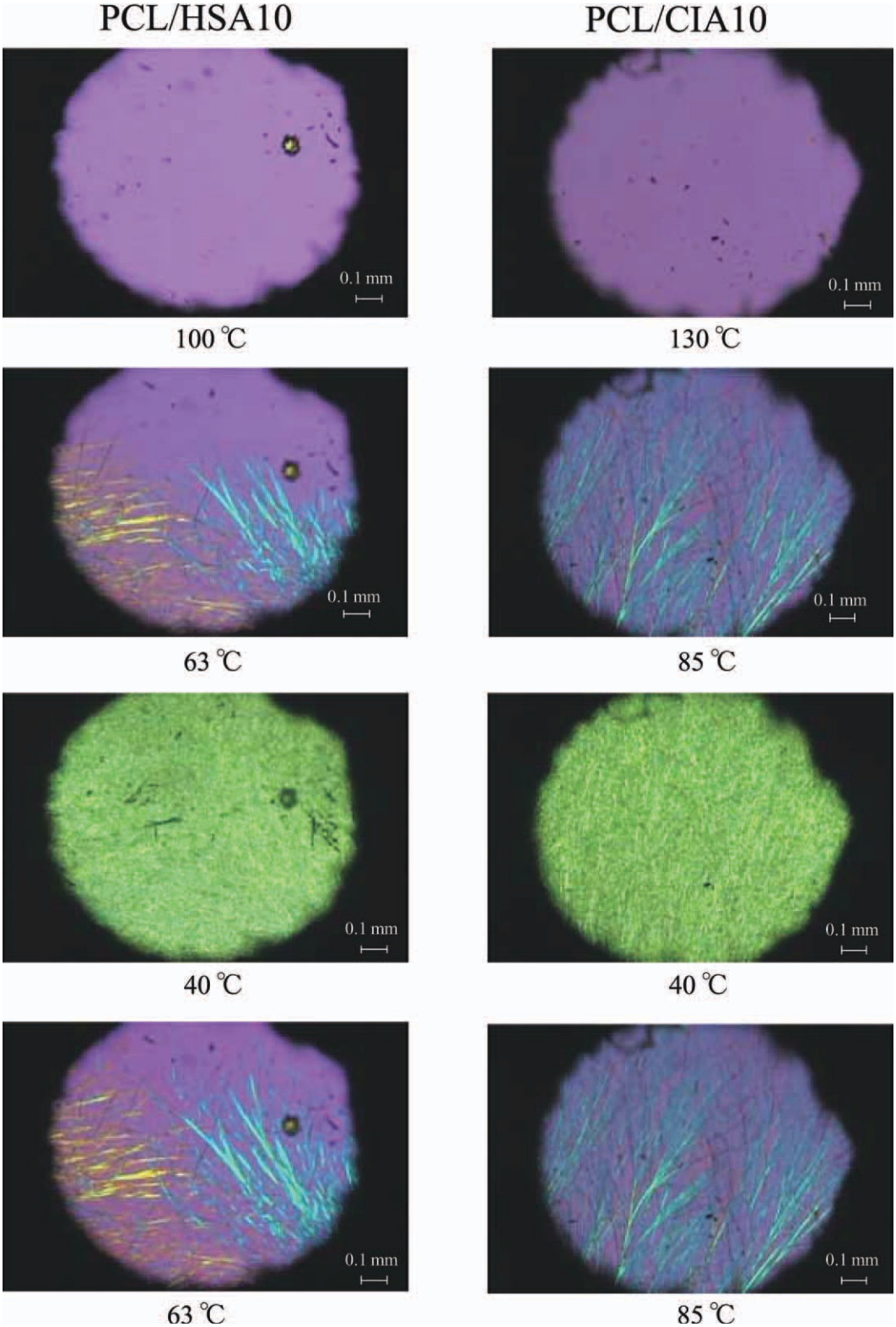

Figure 4 Polarized optical photomicrographs of PCL/HSA10 and PCL/CIA10 at the specified temperature on the cooling stage from 85 to 130°C, respectively at a rate of 1°C/min and the subsequent heating stage from 40°C at a rate of 1°C/min. The time course of the heat treatment is from upper to lower photograph. [Color figure can be viewed in the online issue, which is available at wileyonlinelibrary.com.]

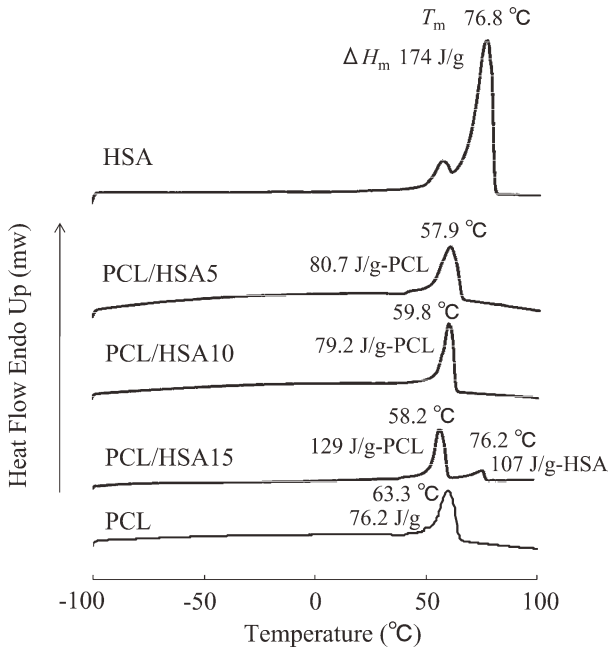

Figure 5 The first heating DSC thermograms of HSA, PCL/HSA5, PCL/HSA10, PCL/HSA15, and PCL.

Mechanical, biodegradable, and remendable properties of PCL/HSA and PCL/CIA cmposites

Figure 9 shows tensile strengths and moduli at 20°C for PCL/HSA, PCL/CIA, and PCL/STA. The tensile strength and modulus of PCL/STA10 was lower than those of PCL. On the other hand, the tensile modulus of PCL/CIA increased with increasing CIA content over the range of 0−15 phr. This result suggests that the CIA fiber with hydrogen bonds has a higher modulus than PCL with covalent bonds. The tensile strength decreased a little with CIA content. Elongation at break of PCL/CIA0, 5, 10, 15 was >300, 18.6, 9.0, and 6.7%, respectively. Therefore, the decrease of tensile strength is related to the increase

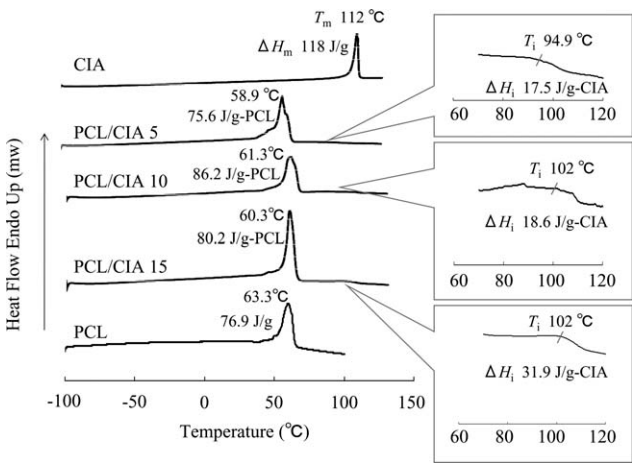

Figure 6 The first heating DSC thermograms of CIA, PCL/CIA5, PCL/CIA10, PCL/CIA15, and PCL.

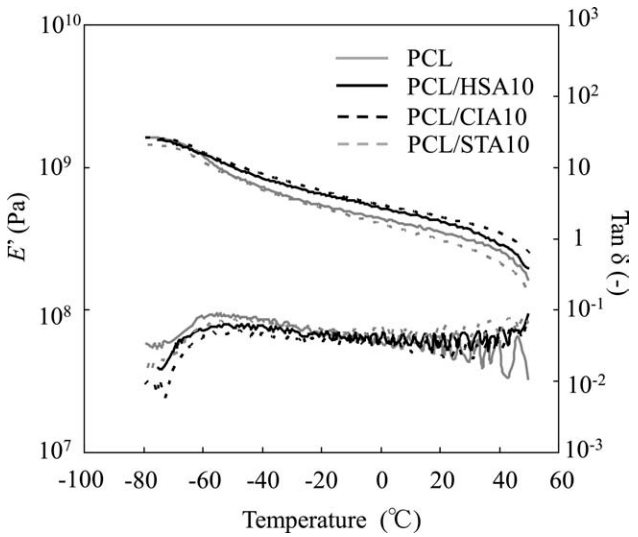

Figure 7 DMA charts of PCL, PCL/HSA10, PCL/CIA10, and PCL/STA10.

of brittleness. The tensile modulus of PCL/HSA also increased with increasing HSA content over the range of 0–10 phr, while dropped at 15 phr, suggesting that HSA mesogenic phase changed to heterogeneous HSA crystalline phase. The tensile strength of PCL/HSA decreased a little with HSA content, corresponding to a decrease of elongation at break (17.6, 14.2, and 10.0% for PCL/HSA5, 10, 15). When the composites with the same LMOG content were compared, the tensile strength of PCL/HSA was higher than that of PCL/CIA. These results suggest that CIA supramolecular fiber based on the hydrogen bonding of highly polar amide groups has a higher modulus and a little more brittle than the HSA fiber based on the hydrogen bonding of carboxylic acid/hydroxyl groups.

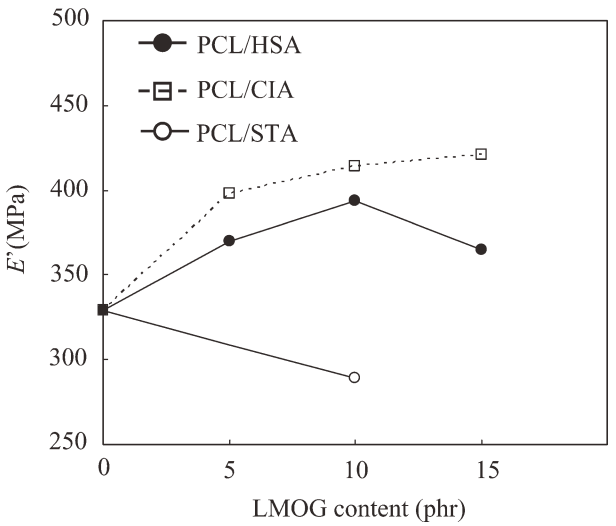

Figure 8 The E' at 20°C measured by DMA for PCL/HSA, PCL/CIA, and PCL/STA with different HSA, CIA, and STA contents.

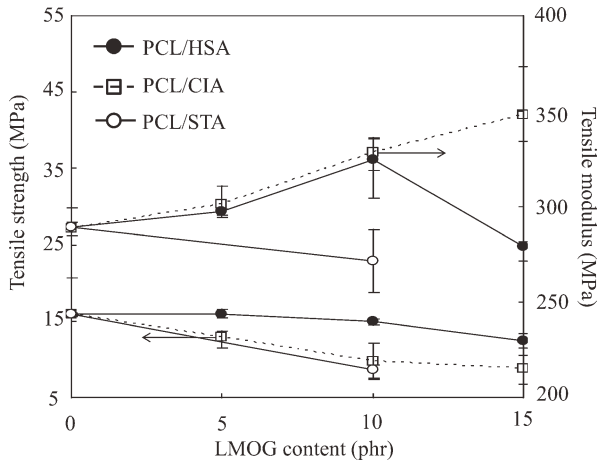

Figure 9 Tensile strength and modulus at 20°C for PCL/HSA, PCL/CIA, and PCL/STA.

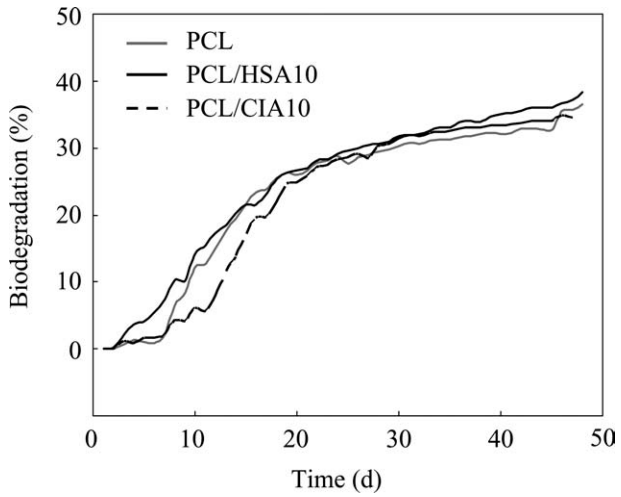

Figure 10 The biodegradability of PCL, PCL/HSA10, and PCL/CIA10 in an aerobic aqueous media with activated sludge measured by BOD method.

Figure 10 shows the biodegradability of PCL/HSA10 and PCL/CIA10 in an aerobic aqueous media with activated sludge measured by BOD method. PCL/HSA10 and PCL/CIA10 showed so high biodegradability as PCL. It is estimated that HSA or CIA has a comparable biodegradability to PCL which has a higher biodegradability than other biodegradable polyesters such as poly(lactic acid) and PBS.[19]

Figure 11 shows the micrographs of regenerated supramolecular fibrous networks of HSA and CIA for PCL/HSA10 and PCL/CIA10 after second

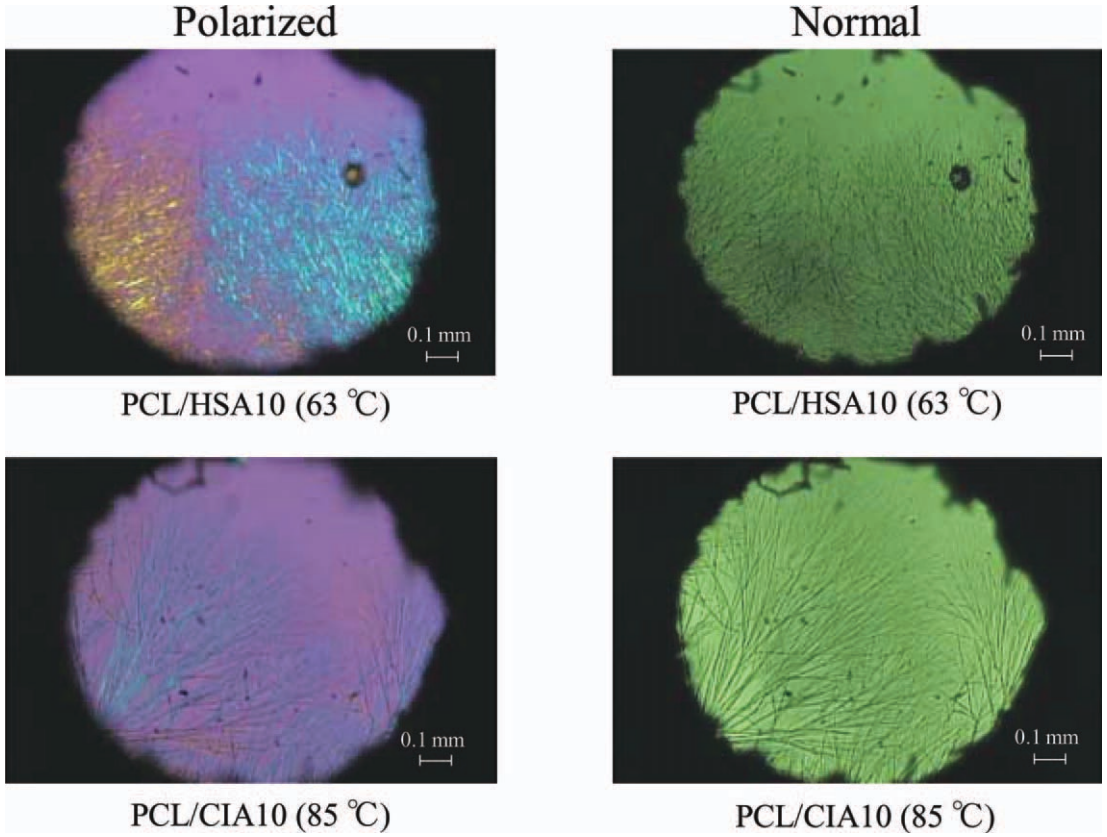

Figure 11 Polarized and normal optical photomicrographs of PCL/HSA10 and PCL/CIA10 at the specified temperature during the second cooling stage from 85 to 130°C at a rate of 1°C/min after the first cooling stage from 85 to 130°C at a rate of 1°C/min and subsequent heating stage from 40°C at a rate of 1°C/min, respectively. [Color figure can be viewed in the online issue, which is available at wileyonlinelibrary.com.]

cooling process at 1°C/min from isotropic liquids at 85 and 130°C, respectively. It is obvious that the fibrous networks of HSA and CIA are again regenerated during the second heating process. The regeneration of the fibrous network could be seen several times when the heat cycle was repeated.

CONCLUSIONS

When a homogeneous hot liquid of PCL with 5–15 phr HSA or CIA was gradually cooled to room temperature, the mixture became gelatinous material and then solidified to give PCL/HSA or PCL/CIA composite. The gelation during the cooling process was confirmed by the rheological measurements of the mixtures of PCL with HSA and CIA. Furthermore, the formation of supramolecular fibrous networks during the cooling process and the maintenance of the networks after crystallization of PCL were directly observed by the polarized and normal optical microscopic analysis. The DSC analysis also supported the formation of mesogenic phase of PCL/CIA, while PCL/HSA did not show clear isotropization temperature of HSA mesogenic phase because of the overlapping with the melting endotherm of PCL. The tensile moduli of both the composites increased with increasing CIA and HSA content, while it decreased exceptionally for PCL/HSA (15 phr) due to the crystallization of HSA. The PCL/CIA composites showed a little higher tensile moduli and lower tensile strengths than the PCL/HSA composites with the same LMOG content. In case of PCL/STA10 blend, both the tensile modulus and strength were lower than those of PCL. The E' measured by DMA showed a similar trend to the tensile modulus. Consequently, homogeneous gelation of LMOG is important for the mechanical reinforcement of PCL, while heterogeneous crystallization does not improve the property. The PCL/HSA and PCL/CIA composites showed so high biodegradability as PCL. Regeneration of fibrous network during the repeated cooling process from the isotropic liquid phase for PCL/HSA and PCL/CIA was confirmed by the microscopic analysis. The supramolecular composites in this study are environmentally benign materials with biodegradable and remendable characteristics, although the mechanical reinforcement effect is not so high.

References

1. Gunatillake, P.; Mayadunne, R.; Adhikari, R. Biotechnol Ann Rev 2006, 12, 301.
2. Okada, M. Prog Polym Sci 2002, 27, 87.
3. Chandra, R.; Rustgi, R. Prog Polym Sci 1998, 23, 1273.
4. Pandey, J. K.; Reddy, K. R.; Kumar, A. P.; Singh, R. P. Polym Degrad Stab 2005, 88, 234.
5. Ray, S. S.; Bousmina, M. Prog Mater Sci 2005, 50, 962.
6. Pavlidou, S.; Papaspyrides, C. D. Prog Polym Sci 2008, 33, 1119.
7. Bordes, P.; Pollet, E.; Avérous, L. Prog Polym Sci 2009, 34, 125.
8. Kiliaris, P.; Paraspyrides, C. D. Prog Polym Sci 2010, 35, 902.
9. Vilaplana, F.; Strömberg, E.; Karlsson, S. Polym Degrad Stab 2010, 95, 2147.
10. Shibata, M.; Teramoto, N.; Kaneko, K. J Polym Sci Part B: Polym Phys 2010, 48, 1281.
11. Sakamoto, K.; Yoshida, R.; Hatano, M.; Tachibana, T. J Am Chem Soc 1978, 100, 6898.
12. Hanabusa, K.; Hiratsuka, K.; Kimura, M.; Shiraim, H. Chem Mater 1999, 11, 649.
13. Suzuki, M.; Sata, T.; Kurose, A.; Shirai, H.; Hanabusa, K. Tetrahedron Lett 2005, 46, 2741.
14. Fu, X.; Wang, N.; Zhang, S.; Wang, H.; Yang, Y. J Colloid Interface Sci 2007, 315, 376.
15. Suzuki, M.; Abe, T.; Hanabusa, K. J Colloid Interface Sci 2010, 341, 69.
16. George, M.; Weiss, R. G. In Molecular Gels: Materials with Self-Assembled Fibrillar Networks; Weiss, R. G., Terech, P., Eds.; Springer: Dordrecht, 2006; Chapter 14, pp 449–552.
17. Liu, X. Y. In Low Molecular Mass Gelators: Design, Self-Assembly, Function; Fages, F., Ed.; Springer: New York, 2005; pp 1–38.
18. Terech, P.; Weiss, R. G. Chem Rev 1997, 97, 3133.
19. Teramoto, N.; Urata, K.; Ozawa, K.; Shibata, M. Polym Degrad Stab 2004, 86, 401.